Impact of shell thickness on exciton and biexciton binding energies of a ZnSe/ZnS core–shell quantum dot

ARTICLE *in* JOURNAL OF PHYSICS AND CHEMISTRY OF SOLIDS · SEPTEMBER 2010

Impact Factor: 1.85 · DOI: 10.1016/j.jpcs.2010.04.014

4 AUTHORS:

Pratima Sen
Devi Ahilya University, Indore
61 PUBLICATIONS **178** CITATIONS
SEE PROFILE

Saikat Chattopadhyay
St. Xaviers College; Jalpaiguri, North Bengal
7 PUBLICATIONS **44** CITATIONS
SEE PROFILE

Joseph Thomas Andrews
Shri Govindram Seksaria Institute of Techn…
45 PUBLICATIONS **208** CITATIONS
SEE PROFILE

Pranay Kumar Sen
Shri Govindram Seksaria Institute of Techn…
180 PUBLICATIONS **1,052** CITATIONS
SEE PROFILE

Journal of Physics and Chemistry of Solids 71 (2010) 1201–1205

Contents lists available at ScienceDirect

Journal of Physics and Chemistry of Solids

journal homepage: www.elsevier.com/locate/jpcs

Impact of shell thickness on exciton and biexciton binding energies of a ZnSe/ZnS core–shell quantum dot

Pratima Sen [a,*], Saikat Chattopadhyay [a], Joseph Thomas Andrews [b], Pranay Kumar Sen [b]

[a] Laser Bhawan, School of Physics, Devi Ahilya University, Indore 452017, India
[b] Department of Applied Physics, Shri G S Institute of Technology & Science, Indore 452003, India

ARTICLE INFO

Article history:
Received 1 December 2009
Received in revised form
22 March 2010
Accepted 9 April 2010

Keywords:
A. Semiconductors
A. Nanostructures
A. Optical materials
D. Electronic structure

ABSTRACT

Impact of shell structure on the exciton and biexciton binding energies has been studied in a ZnSe/ZnS core–shell quantum dot using Wentzel–Kramers–Brillouin (WKB) approximation. For excitons, the binding is caused by the Coulombic as well as the confinement potentials while biexciton binding energy is determined by taking into account the exchange and correlation effects. The exciton binding energy was found to increase initially with increasing shell thickness which reaches saturation at larger shell thickness. On the other hand, the biexciton binding energy exhibits a crossover from the bonding to antibonding state with increasing shell thickness for smaller core radius of the quantum dot.

1. Introduction

Semiconductor quantum dots (QDs) have drawn significant attention in the last couple of decades as they play the role of key materials for modern optoelectronic and spintronic nanodevices [1,2]. In the semiconductor quantum dots, the electrons and holes are confined within the width of a semiconductor layer of lower energy gap which is surrounded by another semiconductor with a higher band gap and is generally lattice matched with the former [3]. The confinements of electrons and holes give rise to novel optical and electronic properties. These nanostructures are popularly known as core–shell quantum dots (CSQDs). It has been experimentally observed that such CSQDs exhibit improved photoluminescence (PL) efficiency over that from the bare quantum dots and the thickness of the shell provides further control on optical and electronic properties of these QDs [4]. Some reported example of CSQD are CdSe/ZnS, ZnS/CdS, CdSe/HgS, CdSe/CdS, ZnSe/ZnS, etc. [5,6].

Of late, Lad and Mahanuni [5] have observed nearly 42% increase in PL intensity due to the presence of ZnS shell around the ZnSe quantum dot. The electronic and optical properties of ZnSe/ZnS and ZnS/ZnSe CSQDs were theoretically studied by Goswami et al. [6] where they found that a charge transfer from core to shell takes place and the core–shell structure exhibits a red shift in the absorption spectra. Growth and PL study of ZnSe QD was also reported by Chang et al. [7] following a flow controlled method for growing ZnSe QDs embedded in ZnS and observed experimentally that for shorter growth time, the QD size was smaller and the blue shift in the PL spectra was larger. The smaller QD size means smaller core radius which corresponds to larger confinement potential and gives rise to blue shift in absorption spectra.

The stimulus for the present work stems from the report of the red shift in the PL spectra as well as the increase in the PL intensity in CSQD due to the presence of shell [4]. In our earlier work [8–11], we reported nonlinear and coherent transient optical properties of a single quantum dot. The energy level structure in the bare QD was also reported by our group [12] as well as by other groups [13–16] taking into account the parabolic, spherical, square well and other types of confinement potential functions. In these models, the spreading of the single particles wavefunctions to the shell was not given due consideration. In our opinion, the inclusion of tunneling property should be incorporated to include the effect of shell on the energy level structures of the core–shell QDs. In the present paper, we have chosen WKB wave functions with due weightage to the boundary conditions at the core/shell interface and calculated the exciton and biexciton binding energies in the CSQDs. The theoretical results exhibit increase in the binding energies of excitons and biexcitons due to the presence of the shell. Consequently, the transition energies also show red shifts as observed by Mahamuni et al. [5] in the PL spectra of CSQD.

2. Theoretical formulations

There are two types of CSQDs. In type-I CSQD, the band offset are such that both electron and hole are confined within the core

* Corresponding author. Tel.: +91 731 2762 153.
E-mail address: pratimasen@gmail.com (P. Sen).

0022-3697/$ - see front matter © 2010 Elsevier Ltd. All rights reserved.
doi:10.1016/j.jpcs.2010.04.014

while in type-II CSQD, only one of the carriers is confined in the core region and the other carrier may extend to the shell region [17]. In ZnSe/ZnS CSQD, ZnS provides strong confinements to the electrons and holes in the core region. It has a higher bulk band gap energy (3.68 eV [18]) than in case of bulk ZnSe (2.8 eV [19]). It is well known that ZnSe/ZnS structure is not lattice matched and forms a strained interface. Shahzad et al. [20] reported the result of optical characterization and band offsets in ZnSe–ZnS_xSe_{1-x} strained layer superlattices. They [20,21] had also presented the theoretical results of the heterojunction band discontinuities in the strained layer system based on local density functional pseudopotential formalism. The valence band offset for strained interfaces was obtained by taking into account the strain Hamiltonian [20] where they incorporated the shift of the center of gravity and splitting of the so-called $P_{3/2}$ valence band due to the tetragonal distortion. The eigenvalues of the strain Hamiltonian were calculated by using the unperturbed wave functions of valence and conduction bands in a zinc-blende type material [20]. Taking into account the strained configuration for a ZnS/ZnSe (0 0 1) interface, the valence and conduction band offset were reported to be 0.58 and 0.03 eV, respectively.

The conduction-band offset for electrons in ZnSe/ZnS is very small and the electrons are loosely bound. Also, the hole is much heavier in the ZnSe core with $m_h^*=0.60m_0$ [4] compared to the hole inside the ZnS shell ($m_h^*=0.49m_0$ [4]). Consequently, in a ZnSe/ZnS CSQD system the electron wave function can spread over the shell as well as core domain but the hole is preferentially localized inside the core area [4]. The electron confinement in such cases is possible for very small QD structures where both Coulomb and confinement potentials are responsible for the binding of the electron–hole pairs.

The geometry of the ZnSe/ZnS QD under consideration is shown in Fig. 1. Here, a is the radius of the core while b is the radius of the CSQD as a whole.

We consider two dimensional confinement potential for electrons (V_e) and holes (V_h) to be of parabolic type such that for $|r|\le a$

$$V_e(r)=\frac{V_c}{a^2}(r^2-a^2) \tag{1}$$

and

$$V_h(r)=\frac{V_v}{a^2}(r^2-a^2). \tag{2}$$

Here, V_c and V_v are the conduction and valence band offsets. We consider that the quasi-particles like electrons and holes in the CSQD experience strong confinement potential within the core due to the presence of the shell. Outside the core region, the particle wave function still remains confined in the shell due to the presence of a buffer layer. Consequently, the particle experiences an overall double confinement like structure. The single particle wave functions under such situation can be described by the WKB wavefunctions given by [22]

$$\phi_j(a,b)=\begin{cases}\dfrac{A_S}{\sqrt{\kappa_j}}\exp\left[\int_{-b}^{-a}\kappa_j\,dr\right] & \text{for} \quad -b<r<-a,\\ \dfrac{A_C}{\sqrt{k_j}}\sin\left[\int_{-a}^{a}k_j\,dr+\dfrac{\pi}{4}\right] & \text{for} \quad -a<r<a,\\ \dfrac{A_S}{\sqrt{\kappa_j}}\exp\left[-\int_{a}^{b}\kappa_j\,dr\right] & \text{for} \quad a<r<b.\end{cases} \tag{3}$$

Here, j stands for electron (e) or hole (h) single particles. A_C and A_S are the normalization constants for core and shell region, respectively, and

$$k_j=\sqrt{1-\frac{\sqrt{m_jV_j}r}{\hbar}} \quad \text{and} \quad \kappa_j=ik_j. \tag{4}$$

For a bare quantum dot, we restrict the value of the running parameter r in the range $-a\le r\le a$ while the contribution of shell is obtained by assigning appropriate values to the running parameter r as $-b\le r\le -a$ and $a\le r\le b$ in the forthcoming calculations. Apart from this, the change in the physical parameters regarding energy and effective mass of electron have been incorporated in the core and shell region. The WKB wavefunctions defined by Eq. (3) are the single particle envelope functions. Under effective mass approximation, the total wavefunctions ψ_e and ψ_h can be written as the product of the envelope function and the Bloch function (u_e, u_h).

$$\psi_e(a,b,r_e)=\phi_e(a,b)\cdot u_e(r_e) \tag{5}$$

and

$$\psi_h(a,b,r_h)=\phi_h(a,b)\cdot u_h(r_h). \tag{6}$$

Here, r_e and r_h represent the position vectors of electron and hole, respectively.

The optical properties of the semiconductor quantum dots are determined by the electron–hole (e–h) pair state called as, exciton. In QDs, the e–h pair formation is influenced by the confinement potential in addition to the Coulombic term. Within Hartree approximation [23], the exciton ground state wavefunction (ψ_X) can be written as

$$\psi_X(a,b,r_e,r_h)=\phi_e(a,b)u_e(r_e)\cdot\phi_h(a,b)u_h(r_h). \tag{7}$$

Using these wavefunctions, the exciton binding energy Δ_X can be calculated as [16]

$$\Delta_X(a,b)=\left\langle\psi_X(a,b,r_e,r_h)\left|\left(V_e+\frac{e^2}{\varepsilon_0 r}\right)\right|\psi_X(a,b,r_e,r_h)\right\rangle + \left\langle\psi_X(a,b,r_e,r_h)\left|\left(V_h+\frac{e^2}{\varepsilon_0 r}\right)\right|\psi_X(a,b,r_e,r_h)\right\rangle. \tag{8}$$

In Fig. 2, we have plotted the variation of exciton binding energy as a function of dot radius in a bare ZnSe QD using Eqs. (3)–(8) for $-a\le r\le a$. The physical parameters chosen for the numerical analysis include the effective mass of electron in ZnSe and ZnS as $m_e^*=0.17m_0$ and $m_e^*=0.39m_0$, respectively [24,25]. The figure exhibits a decrease in exciton binding energy with increasing dot size which is similar to the experimental observations of Chang et al. [7] where they calculated the binding energy from the activation energy.

In order to verify the effect of the shell formation on the binding energy of excitons (Δ_X), we have plotted the variation of

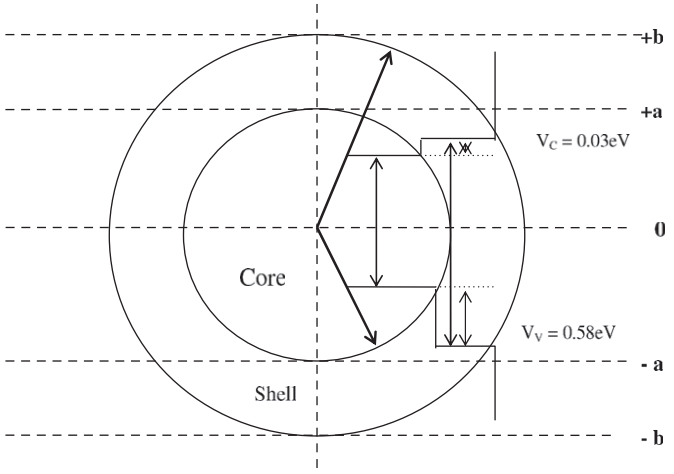

Fig. 1. Schematic of a core–shell quantum dot and dimensions as assumed in the present calculations.

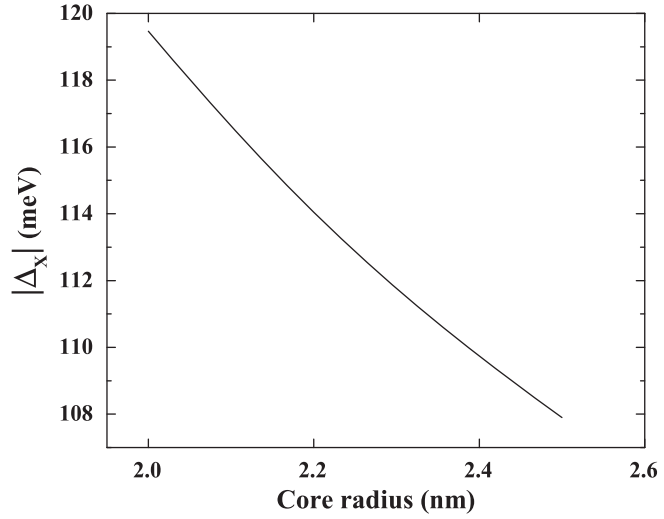

Fig. 2. Variation of the exciton binding energy ($|\Delta_X|$) with dot radius in a bare ZnSe QD.

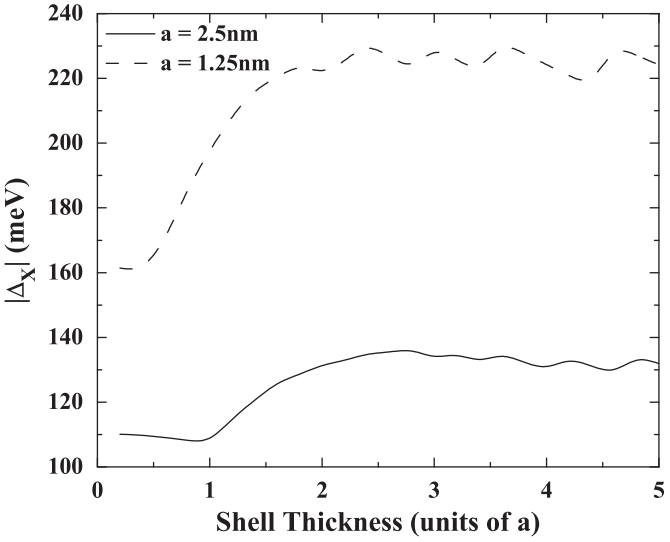

Fig. 3. Dependence of the exciton binding energy ($|\Delta_X|$) on the increasing shell thickness in ZnSe/ZnS core–shell QD.

exciton binding energy as a function of shell thickness in Fig. 3. We have applied the analysis to two CSQDs of core radii 2.5 and 1.25 nm. For each of the CSQDs, the shell width $|b-a|$ is varied from a to $5a$ i.e. nearly 5 times the core radius. This figure clearly illustrates that the presence of shell layer causes an increase in the exciton binding energy for few mono layers of shell thickness. For larger shell thickness, the exciton binding energy saturates. The apparent increase in exciton binding energy is due to the spreading of single particle wave function to the shell region. While examining the effect of ZnS shell thickness on confined energy levels of ZnSe QD, Lad and Mahamuni [5] observed a red shift in the lowest excitonic transition with increase in ZnS shell thickness. The larger red shift shows increase in exciton binding energy which causes reduction in ground-to-exciton level transition energy. In order to make a distinct comparison between the present theoretical results and the experiment, the expression for the red shift $\Delta E(x)$ in the optical absorption spectra as observed by Lad and Mahamuni [5] with increasing shell thickness x is defined as

$$\Delta E(x) = \Delta_x(a,a+x) - \Delta_x(a,a), \tag{9}$$

remembering that the two terms on the right hand side of Eq. (9) stand for the binding energies in case of the CSQD and the bare QD.

In Fig. 4, we have made an attempt to compare the results obtained from the present theoretical analysis with the available experimental results [5] using Eq. (9). For this purpose we have taken the values of the physical parameters and same scaling as used in Ref. [5]. It may be recalled that in the experiment performed by Lad and Mahamuni [5], each monolayer of ZnS has been considered to be of 2 Å thickness. Three figures (a), (b) and (c) plotted in Fig. 4 are for ZnSe core sizes of 43, 33 and 24 Å, respectively and are same as in Ref. [5]. It is evident from this figure that the nature of dependence of the red shift on the ZnS shell thickness as obtained from the present theory is qualitatively in very good agreement with the experimental results. However, all the three figures manifest that the numerical value of the red shift obtained by us is much smaller than the experimental results. This discrepancy can be due to the idealized conditions we have assumed for the core–shell interface in the calculations. More critically, it may be stated that the large number of factors such as lattice mismatch between the core and shell ($\approx 5\%$) and other imperfections like impurities, dislocations etc have been completely overlooked. In a real core–shell quantum dot with finite lattice mismatch, one must include the contribution of the strains in both materials while constructing the pseudomorphic interface [21]. In ZnSe/ZnS QD, ZnSe near the interface will experience a compressive strain while ZnS near the interface will experience expansive strain giving rise to modifications in band alignment [5]. To the authors' knowledge, the present theoretical analysis is first of its kind to study exciton and biexciton binding energy in core–shell quantum dots. Hence, the simplified model yielding result qualitatively in agreement with the experimental observations appear justified.

The decreasing trend in red shift with increasing shell thickness as well as the order of magnitude of red shift matches quite well with the experimental observations. The similarity between our results and that of Lad and Mahamuni [5] confirms that the cause of red shift in absorption spectra is responsible for the spreading of single particle wavefunction to the shell region.

We have further analyzed the effect of shell thickness on biexciton binding energy in a CSQD. The expression for the biexciton binding energy Δ_{XX} is calculated as [26]

$$\begin{aligned}\Delta_{XX}(a,b) = &\left\langle \psi_e(a,b,r_e)\left|\left(V_e+\frac{e^2}{\varepsilon_0 r}\right)\right|\psi_e(a,b,r_e)\right\rangle \\ &-\left\langle \psi_h(a,b,r_h)\left|\left(V_h+\frac{e^2}{\varepsilon_0 r}\right)\right|\psi_h(a,b,r_h)\right\rangle \\ &+\left\langle \psi_e(a,b,r_e)\left|\left(V_h+\frac{e^2}{\varepsilon_0 r}\right)\right|\psi_e(a,b,r_e)\right\rangle \\ &-\left\langle \psi_h(a,b,r_h)\left|\left(V_e+\frac{e^2}{\varepsilon_0 r}\right)\right|\psi_h(a,b,r_h)\right\rangle. \end{aligned} \tag{10}$$

The positive (negative) values of Δ_{XX} indicate bonding (antibonding) biexciton energy states [26]. The calculations were made for a bare QD as well as a CSQD. The variation in biexciton binding energy as a function of dot radius has been plotted for a bare QD using Eqs. (3)–(10) in Fig. 5. This figure indicates that in a bare QD, the biexciton binding energy decreases with decreasing dot size. While studying fine structure splitting and biexciton binding energy in single self assembled InAs/AlAs QD, Sarkar et al. [27] also experimentally observed similar variation. The reduction in the binding energy reflects a possible crossover to the antibonding regime. The influence of shell thickness on biexciton binding energy has been plotted in Fig. 6 for two different values of the core radius. We find that the biexciton

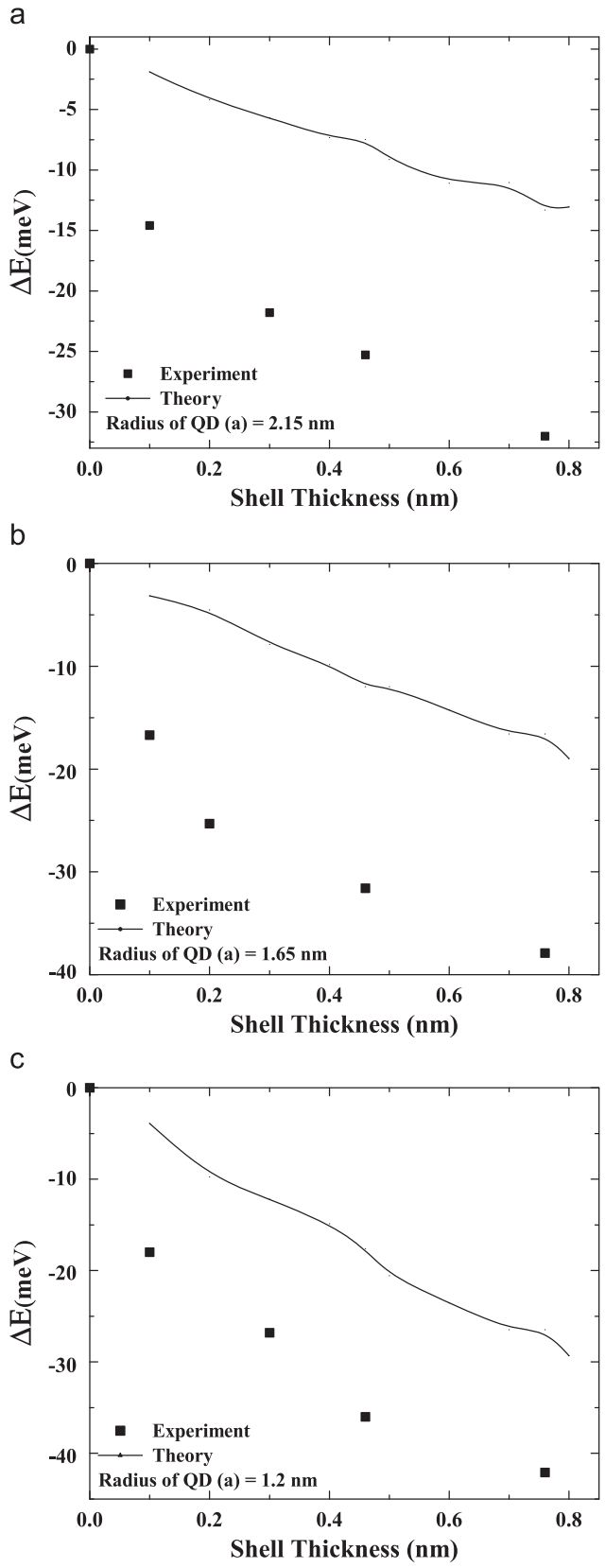

Fig. 4. Variation in the red shifts ($\Delta E(x)$) with shell thickness (x) of the present analysis with the experimental results in ZnSe/ZnS core–shell QD with different core radii; (a) core radius =2.15 nm, (b) core radius =1.65 nm, (c) core radius =1.2 nm.

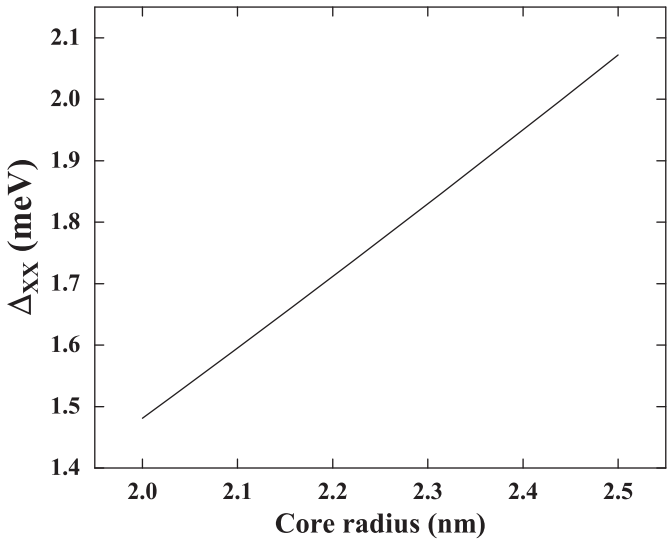

Fig. 5. Variation of the biexciton binding energy (Δ_{XX}) with dot radius in a bare ZnSe QD.

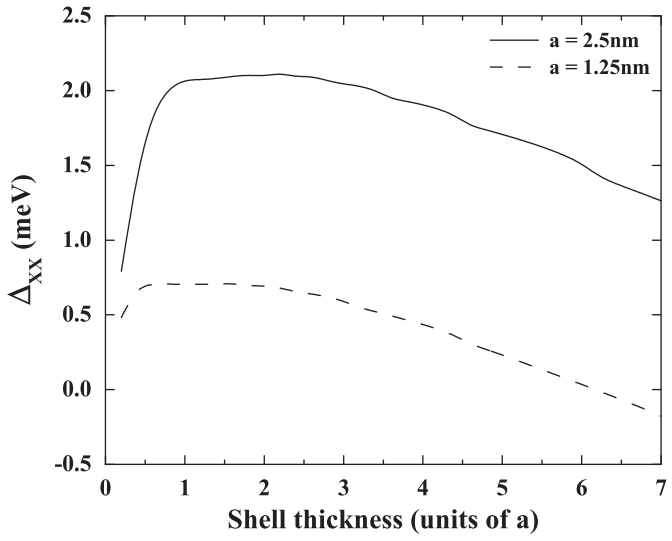

Fig. 6. Dependence of the biexciton binding energy (Δ_{XX}) on the shell thickness in ZnSe/ZnS core–shell QD.

binding energy decreases sharply with increasing shell thickness. In the QD of smaller core radius (1.25 nm), the biexciton attains an antibonding state beyond a shell width of 6a. The antibonding biexciton state appears due to the fact that the hole confinement becomes stronger and leads to an enhancement in the hole–hole interaction represented by the last term in Eq. (10). The strong hole–hole interaction indicates an increase in the repulsive force and causes antibonding of biexcitons.

3. Conclusions

In conclusion, we find that in a conventional core shell semiconductor QD, the electron and hole wavefunctions are modified inside the core area due to the presence of the shell layer. The present analysis based upon the WKB approximation method is appropriate to select the modified wavefunctions for the electrons and holes as it explains the experimentally observed increase in exciton binding energy due to the presence of the

shell. The theory also explains successfully the bonding and antibonding states of biexcitons in core–shell quantum dots.

Acknowledgement

The financial support received from Department of Science & Technology (DST), New Delhi, India, is gratefully acknowledged.

References

[1] S. Dutta, B. Das, Electronic analog of the electro-optic modulator, Appl. Phys. Lett. 56 (1990) 665.
[2] H.M. Gibbs, Optical Bistability: Controlling Light with Light, Academic Press, Orlando, 1985.
[3] L. Jacak, P. Hawrylak, A. Wojs, Quantum Dots, Springer, Berlin, 1998.
[4] V.V. Nikesh, S. Mahamuni, Highly photoluminescent ZnSe/ZnS quantum dots, Semicond. Sci. Technol. 16 (2001) 687.
[5] A. Lad, S. Mahamuni, Effect of ZnS shell formation on the confined energy levels of ZnSe quantum dots, Phys. Rev. B 78 (2008) 125421.
[6] B. Goswami, S. Pal, P. Sarkar, A theoretical study on the electronic structure of ZnSe/ZnS core/shell nanoparticles, J. Phys. Chem. C 112 (2008) 11630.
[7] Y.H. Chang, M.H. Chieng, C.C. Tsai, M.C. Harris Liao, Y.F. Chen, Growth and photoluminescence study of ZnSe quantum dots, J. Elect. Mat. 29 (2000) 173.
[8] J.T. Andrews, P. Sen, Steady state optical gain in small semiconductor quantum dots, J. Appl. Phys. 91 (2002) 2827.
[9] P. Sen, J.T. Andrews, Nonlinear absorption in semiconductor quantum dots, Solid State Commun. 120 (2001) 195.
[10] M.K. Bafna, P. Sen, P.K. Sen, Temperature dependence of the photoluminescence properties of self-assembled InGaAs/GaAs single quantum dot, J. Appl. Phys. 100 (2006) 103515.
[11] J.T. Andrews, P. Sen, R.R. Puri, Optical absorption spectra of a quantum dot in a microcavity, J. Phys. Condens. Matter 11 (1999) 6287.
[12] J. Kumar, S. Kapoor, S.K. Gupta, P.K. Sen, Theoretical investigation of the effect of asymmetry on optical anisotropy and electronic structure of Stranski–Krastanov quantum dots, Phys. Rev. B 74 (2006) 115326.
[13] Al.L. Efros, Luminescence polarization of CdSe microcrystal, Phys. Rev. B 46 (1992) 7448.
[14] M. Nirmal, D.J. Norris, M. Kuno, M.G. Bawendi, Al.L. Efros, M. Rosen, Phys. Rev. Lett. 75 (1995) 3728.
[15] J.H. Davies, The Physics of Low-dimensional Semiconductors an Introduction, Cambridge University Press, New York, 1998, pp. 118-146.
[16] L. Banyai, S.W. Koch, Semiconductor Quantum Dots, first ed., World Scientific, Singapore, 1993, pp. 116–149.
[17] S. Kim, B. Fisher, H.J. Eisler, M. Bawendi, J. Am. Chem. Soc. 125 (2003) 11466.
[18] N. Kumbhojkar, V.V. Nikesh, A. Kshirsagar, S. Mahamuni, Photophysical properties of ZnS nanoclusters, J. Appl. Phys. 88 (2000) 6260.
[19] D.J. Chadi, Doping in ZnSe, ZnTe, MgSe and MgTe wide-band-gap semiconductors, Phys. Rev. Lett. 72 (1994) 534.
[20] K. Shahzad, D.J. Olego, C.G. Van de Walle, Optical characterization and band offsets in ZnSe–ZnS_xSe_{1-x} strained-layer superlattices, Phys. Rev. B 38 (1988) 1417.
[21] C.G. Van de Walle, Band lineups and deformation potentials in the model-solid theory, Phys. Rev. B 39 (1989) 1871.
[22] A. Ghatak, S. Lokanathan, Quantum Mechanics Theory and Applications, fifth ed., Macmillan India Ltd., New Delhi, 2004, pp. 380-410.
[23] O. Madelung, Introduction to Solid State Theory, third ed., vol. 2, Berlin, 1996.
[24] D.T.F. Marple, Refractive index of ZnSe, ZnTe and CdTe, J. Appl. Phys. 35 (1964) 539.
[25] L.I. Berger, Semiconductor Materials. CRC Press, Florida, 1997, p. 186.
[26] M. Grundmann (Ed.), Nano-optoelectronics Concepts, Physics and Devices, Springer-Verlag, Berlin, 2002, pp. 181–182.
[27] D. Sarkar, H.P. Van der Meulen, J.M. Calleja, J.M. Becker, R.J. Haug, K. Pierz, Fine structure splitting and biexciton binding energy in single self-assembled InAs/AlAs quantum dots, Physica E 32 (2006) 111.